



ELSEVIER

Astroparticle Physics 14 (2000) 7–13

Astroparticle
Physics

www.elsevier.nl/locate/astropart

Energy estimation of UHE cosmic rays using the atmospheric fluorescence technique

C. Song^{a,*}, Z. Cao^b, B.R. Dawson^c, B.E. Fick^d, P. Sokolsky^b, X. Zhang^a^a Department of Physics, Columbia University, New York, NY 10027, USA^b High Energy Astrophysics Institute, University of Utah, Salt Lake City, UT 84112, USA^c University of Adelaide, Adelaide, SA 5005, Australia^d Enrico Fermi Institute, University of Chicago, Chicago, IL 60637, USA

Received 11 October 1999; accepted 22 December 1999

Abstract

We use the CORSIKA air shower simulation program to review the method for assigning energies to ultra-high energy cosmic rays viewed with the air fluorescence technique. This technique uses the atmosphere as a calorimeter, and we determine the corrections that must be made to the calorimetric energy to yield the primary cosmic-ray energy. © 2000 Elsevier Science B.V. All rights reserved.

PACS: 96.40.Pq; 13.85.Tp

Keywords: Cosmic rays; Energy estimation; Fluorescence light

1. Introduction

One of the goals in a cosmic-ray detection experiment is to determine the energy of the incident particles. Unfortunately, the primary energy cannot be measured directly at high energies, where the flux is very low. Instead, we take advantage of the cascades (or extensive air showers) produced by the cosmic rays in the atmosphere. The secondary particles that make up the cascade can be detected at ground level, as can the Čerenkov light that they produce. Alternatively, one can detect the atmospheric nitrogen fluorescence light in-

duced by the passage of the shower. This technique, employed by the Fly's Eye detector and its successor the high resolution Fly's Eye (HiRes) has the advantage that one can measure the number of charged particles in the shower as a function of depth in the atmosphere, $N_{\text{ch}}(X)$, where X is measured in g/cm^2 . We treat the atmosphere as a calorimeter, and the primary cosmic-ray energy can be estimated by integrating the longitudinal profile $N_{\text{ch}}(X)$ and making corrections for "unseen" energy.

In the past, the energy of a pure electromagnetic shower has been determined by [2]

$$E_{\text{em}} = \frac{E_c}{X_0} \int_0^\infty N_e(X) dX, \quad (1)$$

where X_0 is the electron radiation length in air, E_c is the critical energy of an electron in air, and N_e is

* Corresponding author. Tel.: +1-801-581-4306; fax: +1-801-581-6256. Present address: 115S. 1400E. #201, Dept. of Physics, Univ. of Utah, Salt Lake City, UT 84112, USA.

E-mail address: csong@cosmic.utah.edu (C. Song).

the number of electrons in the shower. This equation implies that the electromagnetic energy is the total track length of all charged particles multiplied by an energy loss rate dE/dX given by E_c/X_0 . One source of error here is the numerical value of the critical energy E_c , which has two definitions attributed to Rossi [5], and Berger and Seltzer [6]. We turn to simulations to check the result and avoid this confusion.

We do this using the modern shower simulation package CORSIKA [1]. We simulate ultra-high energy showers, complete with realistic fluctuations and realistic distributions of the energies of shower particles. An example is shown in Fig. 1, where we plot the energy spectra of shower particles at the depth of the maximum size. Particle energies cover a wide range and lose energy to ionization at different rates (see the inset of the figure).

For these simulations, we replace Eq. (1) with a more general expression for the calorimetric energy

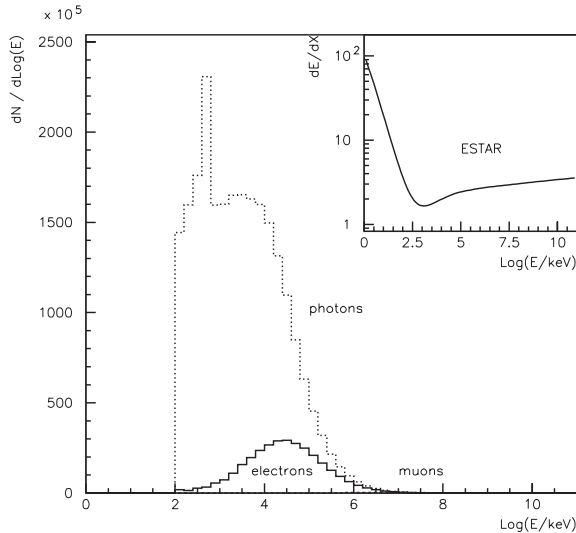


Fig. 1. The mean energy spectra of photons, electrons and muons at $S = 1$ for 200 proton showers at 10^{17} eV. The spike in the photon spectrum corresponds to electron–positron annihilation. The inset shows the energy-loss rate (in MeV/g/cm²) by ionization of electrons in dry air over the same energy range as the main figure. The ESTAR code produced by the US National Institute of Science and Technology (NIST) was used below 10 GeV [10] and this curve is extrapolated into the region above 10 GeV.

$$E_{\text{cal}} = \alpha \int_0^{\infty} N_{\text{ch}}(X) dX, \quad (2)$$

where we integrate the charged particle longitudinal profile. We replace the constant in Eq. (1) with a parameter, α , representing the mean ionization loss rate over the entire shower. (This factor will be approximately equal to E_c/X_0 and is calculated below.) Given E_{cal} , we must then make a correction to determine the cosmic-ray energy E_0 . The correction takes account of the energy carried by high energy muons and neutrinos that ultimately deposit most of their energy in the ground. It also takes account of the small amount of energy that is lost to nuclear excitation. This “missing” energy has previously been parametrized by Linsley [7] and the Fly’s Eye group [8].

In this article, we first describe some characteristics of the CORSIKA shower-simulation package. We then use CORSIKA to simulate γ -ray induced air showers (which have a very small “missing energy” component) to check the calorimetric energy method. Finally, we simulate proton- and iron-induced showers to calculate the “missing energy” corrections for primary energies up to 10^{20} eV.

2. The simulations

CORSIKA is a versatile package for simulating air showers over a wide range of primary energies. Choices are available for the hadronic interaction model at the highest energies, and we have chosen the QGSJET [11] description which is in good agreement with Fly’s-Eye measurements. Within CORSIKA electromagnetic sub-showers are simulated with the EGS4 code [3,4]. In EGS4, the cross sections and branching ratios are extended to 10^{20} eV with the assumption that QED is valid for these energies. In order to reduce the CPU time, a thinning algorithm was selected within CORSIKA. That is, if the total energy of secondary particles from a given interaction falls below 10^{-5} of the primary energy, only one of the secondaries is followed, selected at random according to its energy E_i with a probability of $p_i = E_i/\sum_j E_j$. The sum does not include neutrinos or particles with ener-

gies below the preset thresholds. In our simulations the threshold energies are 300, 700, 0.1 and 0.1 MeV for hadrons, muons, electrons and photons, respectively. Particles below the threshold energies are not followed by the simulation. We chose an observation level 300 m above sea level and, we simulated showers with zenith angles of 45°.

3. Calorimetric energy of an air shower

Consider a purely electromagnetic shower. The primary particle energy E_{em} can be approximated by

$$E_{\text{em}} \cong \int_{\epsilon}^{\infty} \Delta E(k) \mathcal{N}_e(k) dk, \quad (3)$$

where $\mathcal{N}_e(k)$ is the differential energy spectrum of electrons with kinetic energy k , and $\Delta E(k)$ is the energy loss by each of those electrons in the calorimeter via ionization. This is only an approximation because, we have only included particles with kinetic energies above a threshold ϵ . This is consistent with our simulations, where we must impose a threshold of 0.1 MeV for photons, electrons and positrons. This integral can be carried out by summing over all the electrons produced in the simulation.

We rearrange Eq. (3) and include the energy spectrum of particles as a function of atmospheric depth

$$\mathcal{N}_e(k) = \int_0^{\infty} N_e(X) n_e(k, X) \frac{dX}{\Delta X(k)} \quad (4)$$

where $\Delta X(k)$ is the mean free path of electrons as a function of k , $N_e(X)$, the total number of electrons at depth X , and, $n_e(k, X)$, the normalized electron energy spectrum. Then, the electromagnetic energy is approximated by

$$E_{\text{em}} \cong \int_0^{\infty} N_e(X) \left(\int_{\epsilon}^{\infty} \frac{\Delta E}{\Delta X}(k) n_e(k, X) dk \right) dX. \quad (5)$$

The *age* parameter rather than the depth is often used to describe the stage of development of a shower. The energy spectrum of electrons can then

be parametrized in terms of age. Since the age parameter is really only valid for a pure electromagnetic cascade, and as we will use the parameter in reference to hadronic showers, we will refer to our parameter as the *pseudo age*. We define it as

$$S(X) = \frac{3(X - X_1)}{(X - X_1) + 2(X_{\text{max}} - X_1)}, \quad (6)$$

where X_1 is the depth of first interaction and X_{max} is the depth at which the shower reaches maximum size. Under this definition $S(X_1) = 0$, $S(X_{\text{max}}) = 1$ and $S(\infty) = 3$.

One can then calculate the mean ionization loss rate (dE/dX) for the electrons in the shower (with energies $> \epsilon$) at age S

$$\alpha(S) = \int_{\epsilon}^{\infty} \frac{\Delta E}{\Delta X}(k) \tilde{n}_e(k, S) dk, \quad (7)$$

where \tilde{n}_e is now a function of S . For comparison with Eq. (1), we rewrite Eq. (5) as

$$E_{\text{em}} \cong \langle \alpha \rangle_S \int_0^{\infty} N_e(X) dX, \quad (8)$$

where

$$\langle \alpha \rangle_S = \frac{\sum_i \langle N_e \rangle_{\Delta S_i} \alpha(S)_{\Delta S_i}}{\sum_i \langle N_e \rangle_{\Delta S_i}}, \quad (9)$$

and $\langle N_e \rangle_{\Delta S_i}$ is the average number of electrons within a *pseudo age* bin ΔS_i .

We have simulated 10^{17} eV showers initiated by photons, protons and iron nuclei in order to calculate the mean energy loss rate over the entire shower, $\langle \alpha \rangle_S$. We use bins of $\Delta S_i = 0.1$. Fig. 2 shows $\alpha(S)$ as a function of age and, we find $\langle \alpha \rangle_S$ is 2.186, 2.193 and 2.189 MeV/(g/cm²) for gamma, proton and iron induced showers, respectively. All the errors in those $\langle \alpha \rangle_S$ are less than 0.1%.

This compares with the value of the ratio $E_c/X_0 = 2.18$ MeV/(g/cm²) used by Fly's-Eye analysis, where the values were taken to be $E_c = 81$ MeV and $X_0 = 37.1$ g/cm² [12]. This agreement may be a coincidence, since more recent values of

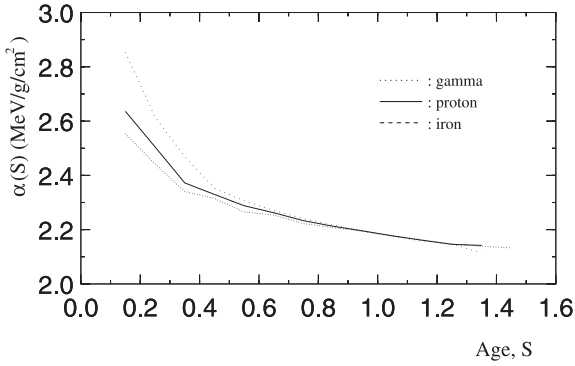


Fig. 2. The mean ionization loss rate dE/dX as function of S for γ -ray, proton, and iron-induced showers at 10^{17} eV.

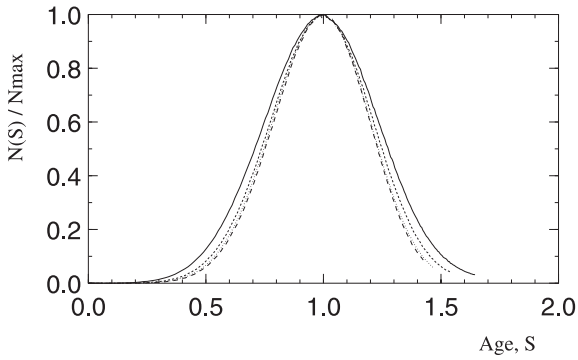


Fig. 3. The solid line indicates the average shower profile for 200 iron induced showers at 10^{17} eV. The other three lines are the average shower profiles for 200 proton showers at 10^{17} eV (---), 10^{18} eV (···) and 10^{19} eV (-·-·).

the parameters from [5] are $E_c = 86$ MeV (using Rossi's definition) and $X_0 = 36.7$ g/cm², giving a ratio which is 7% higher than the typical simulation value of $\langle\alpha\rangle_S$. However, we note that the simulation results only include the energy

loss rates for particles above the 0.1 MeV threshold.

Fig. 3 shows average shower profiles as a function of age for different primary masses and energies, with the shower size normalized to 1, at $S = 1$. The difference in the average proton-induced shower profile at three different primary energies is smaller than the difference between the proton and iron average profiles at one energy. In other words, the shape of the shower development curve as a function of S is quite independent of primary energy or primary mass. It is also well known that for photon primaries the energy spectrum of the shower particles is a function of S only. We found it is also true for hadronic showers in our Monte Carlo study. Hence, we can assume that our result for $\langle\alpha\rangle_S$ can be applied over a range of primary masses and energies.

We now apply Eq. (2) to some γ -ray initiated CORSIKA showers, with $\alpha = 2.19$ MeV/(g/cm²). The CORSIKA energy thresholds are set as described above with a threshold energy of 0.1 MeV for photons, electrons and positrons. We integrate the shower development curves in two ways for comparison. In the first approach, we numerically integrate the CORSIKA output which bins the development curve in 5 g/cm² increments. Alternatively, we fit a Gaisser–Hillas function (with variables X_0 , X_{\max} , N_{\max} and λ) to the CORSIKA output then integrate the function. Both the methods give results which agree at a level of better than 1%.

Table 1 shows the results for 500 showers. The calorimetric energy is about 10% lower than the true value. This is true even when we switch off processes which are not purely electromagnetic,

Table 1
Results of CORSIKA simulations of γ -ray-induced air showers at three primary energies

E_0 (eV)	With $\mu^+\mu^-$ and γN			Without $\mu^+\mu^-$ and γN		
	E_{cal}/E_0	N_μ	N_{max}	E_{cal}/E_0	N_μ	N_{max}
10^{16}	0.888 ± 0.004	$(2.146 \pm 0.795)10^3$	$(8.324 \pm 0.392)10^6$	0.897 ± 0.003	0.000 ± 0.000	$(8.448 \pm 0.413)10^6$
10^{17}	0.888 ± 0.005	$(2.823 \pm 1.369)10^4$	$(7.881 \pm 0.339)10^7$	0.898 ± 0.004	0.000 ± 0.000	$(7.967 \pm 0.392)10^7$
10^{18}	0.889 ± 0.004	$(3.185 \pm 0.916)10^5$	$(7.439 \pm 0.271)10^8$	0.898 ± 0.003	0.000 ± 0.000	$(7.558 \pm 0.281)10^8$

The right side of the table shows the results from simulations where photo-nuclear and muon pair production processes have been switched off. The uncertainties shown are rms errors.

namely the $\mu^+\mu^-$ pair production and photo-nuclear reactions, which have small but important cross sections in γ -ray initiated showers. Two hundred such showers were generated and the results are also shown in Table 1, where we see that these showers have no muon content as expected. However, the deficit in the calorimetric energy remains close to 10%.

The solution to the problem is related to the simulation energy threshold of 0.1 MeV. We have made a detailed study with CORSIKA of the energy-loss mechanisms and the characteristics of particles around 0.1 MeV. In particular, we have summed the energy of particles that drop below the 0.1 MeV threshold. Table 2 shows that at 10^{17} eV, 88.4% of the primary energy is lost to the atmosphere through ionization by particles above 0.1 MeV. Electrons in the shower with energies below 0.1 MeV carry 9.0% of the primary energy, whereas sub-0.1 MeV photons carry 1.2% of the primary energy. The calorimetric energy derived by Eq. (2) is 88.8% of the primary energy: a good match to the ionization energy loss by particles above 0.1 MeV.

We assume that the sub-0.1 MeV particles will eventually lose energy to ionization. The nitrogen fluorescence efficiency is proportional to the ionization loss rate, so experiments like HiRes will detect light in proportion to the energy loss, even for very low-energy particles. Thus, the problem, we experience with reconstructing the energy of CORSIKA simulations will not occur with the real shower data. So, for the further CORSIKA studies described below, we have added 10% of the primary energy to the integrated energy-loss result (from Eq. (2)) to take account of the sub-0.1 MeV particles that do not appear in the CORSIKA output.

4. Energy estimation for hadronic showers

We have described the calorimetric energy estimation for γ -ray induced showers. We next consider hadronic showers, where we expect the calorimetric energy to fall short of the primary energy because of the so-called “missing energy” – the energy channeled into neutrinos, high energy muons, and nuclear excitation. Much of this energy is deposited into the ground and is not visible in the atmospheric calorimeter. The first estimate of missing energy was obtained by Linsley [7] who made measurements of the electron and muon sizes at the ground level and assessed the energy content of these components. The Fly’s-Eye group parametrized Linsley’s estimates as [8]

$$E_{\text{cal}}/E_0 = 0.990 - 0.0782E_0^{-0.175}, \quad (10)$$

where E_0 is the primary energy and E_{cal} is the calorimetric energy derived from Eq. (2), both in units of 10^{18} eV. This parametrization was said to be valid for 10^{15} eV $< E_0 < 10^{20}$ eV.

We have simulated proton and iron initiated showers at eight primary energies from 3×10^{16} to 10^{20} eV using CORSIKA. We apply Eq. (2) (with a mean energy loss rate of 2.19 MeV/(g/cm²)) by fitting a Gaisser–Hillas profile to the CORSIKA development curve and extrapolating the profile to infinity and then integrating the function. We then add 10% of the primary energy to this result to take account of the CORSIKA threshold effect. Finally, we compare this calorimetric energy with the primary energy, as shown in Fig. 4. It is physically reasonable that the missing energy should decrease with increasing primary energy. Because of relativistic effects, charged pions produced in more energetic showers have an increased

Table 2

Results from a study of energy conservation within CORSIKA. γ -ray showers were simulated at three primary energies E_0

E_0 (eV)	E_{loss}/E_0	$E_e (< 0.1 \text{ MeV})/E_0$	$E_\gamma (< 0.1 \text{ MeV})/E_0$	E_{cal}/E_0
10^{16}	0.888 ± 0.003	0.090 ± 0.001	0.010 ± 0.001	0.888 ± 0.004
10^{17}	0.884 ± 0.005	0.090 ± 0.001	0.012 ± 0.003	0.888 ± 0.005
10^{18}	0.876 ± 0.007	0.092 ± 0.002	0.018 ± 0.005	0.889 ± 0.004

E_{loss} refers to the energy lost to the atmosphere through ionization by charged particles with energies above 0.1 MeV. The fraction of the primary energy carried by sub-0.1 MeV electrons and photons is shown in the next two columns. The fraction of primary energy determined by the calorimetric equation (final column) is consistent with E_{loss}/E_0 . Again, all uncertainties are rms.

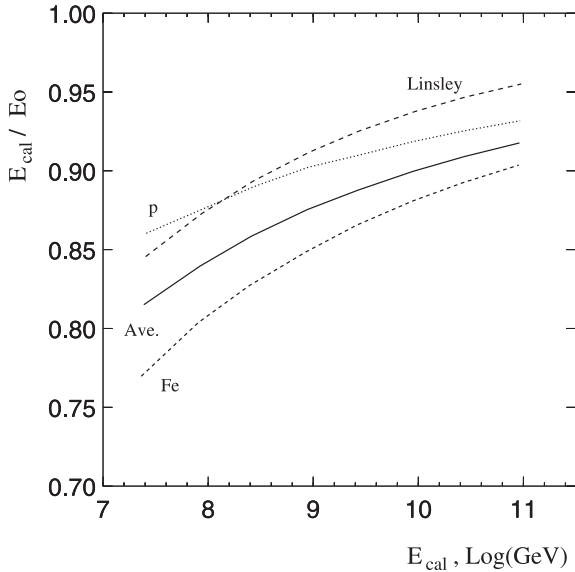


Fig. 4. The functions for correcting the calorimetric energy to the primary energy, as a function of calorimetric energy. Shown are the corrections for proton showers (\cdots) and iron showers ($---$) and the average of the two ($—$). For comparison, Linsley's function is also shown.

chance of interacting rather than suffering decay, reducing the fraction of energy immediately directed into muon and neutrino production. For comparison, we also show Linsley's result. The solid line in Fig. 4 shows the average behavior for proton and iron showers, which we express here as a function of E_{cal} (for practical convenience) in units of 10^{18} eV,

$$E_{\text{cal}}/E_0 = (0.959 \pm 0.003) - (0.082 \pm 0.003)E_{\text{cal}}^{-(0.150 \pm 0.006)}, \quad (11)$$

which is valid for 3×10^{16} eV $< E_0 < 10^{20}$ eV. Unfortunately, it is never possible to know the primary particle mass on a shower-by-shower basis, so this average correction must be used. This lack of knowledge translates into an energy uncertainty, which is at most about 5% if the primary is hadronic. If the primary particle is a γ -ray, this assumption will overestimate the energy by up to 20%. Of course, if the shower-development profile is obviously anomalous (as expected for γ -ray showers above 10^{19} eV due to the LPM effect)

γ -ray primaries can be recognized and this systematic can be avoided.

In an experiment such as HiRes, atmospheric nitrogen fluorescence provides a measurement of ionization energy deposition, since the yield of fluorescence photons is proportional to this energy deposition [9]. In the reconstruction process, we convert the amount of light emitted by the shower at a particular depth to a number of charged particles, assuming that those charged particles ionize at the mean ionization rate which is a function of temperature and density [9]. This is taken into account in our analysis of real showers when we calculate the number of ionizing particles at a particular atmospheric depth. We then perform the path-length integral (Eq. (2)), multiply by the mean ionization loss rate of 2.19 MeV/(g/cm²) and then make a correction for missing energy (Eq. 11).

5. Conclusion

We have re-investigated the veracity of estimating cosmic-ray energy by using the atmosphere as a calorimeter. We have determined that, provided we use an appropriate mean energy loss rate, the technique provides a good estimate of the primary energy for γ -ray induced showers. For hadronic showers, we have derived a correction function which accounts for energy not deposited in the atmosphere, so that the technique also returns a good estimate of primary energy for these showers.

Acknowledgements

We are grateful to Dieter Heck for valuable answers to our questions about CORSIKA. The support from the Center for High Performance Computing at the University of Utah is gratefully acknowledged.

References

- [1] D. Heck, J. Knapp, J.N. Capdevielle, G. Schatz, T. Thouw. CORSIKA: A Monte-Carlo Code to Simulate Extensive Air Showers, Report FZKA 6019, 1998, Forschungszentrum Karlsruhe.

- [2] B. Rossi, *High Energy Particles*, Prentice-Hall, Englewood Cliffs, NJ, 1952 (chapter 5).
- [3] A.F. Bielajew, Photon Monte-Carlo simulation, Report PIRS-0393, National Research Council of Canada, 1993 (<http://ehssun.lbl.gov/egs/epub.html>).
- [4] A.F. Bielajew, D.W.O. Rogers, Electron Monte-Carlo Simulation, Report PIRS-0394, National Research Council of Canada, 1993 (<http://ehssun.lbl.gov/egs/epub.html>).
- [5] Particle Data Group, Review of particle physics, *The Eur. Physical J.* 3 (1998) (76) 148.
- [6] M.J. Berger, S.M. Seltzer, Table of Energy Losses and Ranges of Electrons and Positrons, National Aeronautics and Space Administration Report NASA-SP-3012, Washington DC, 1964.
- [7] J. Linsley, Proc. 18th ICRC, vol. 12, Bangalore, India, 1983, p. 144.
- [8] R.M. Baltrusaitis, et al., Proc. 19th ICRC, vol. 7, La Jolla, USA, 1985, p. 159.
- [9] F. Kakimoto, et al., *Nucl. Instr. Meth. A* 372 (1996) 527.
- [10] M.J. Berger, ESTAR: Computer Program for Calculating Stopping Power, NIST Report NISTIR-4999, Washington DC, 1992 (<http://physics.nist.gov/PhysRefData/Star/Text/ESTAR.html>).
- [11] N.N. Kalmykov, S.S. Ostapchenko, A.I. Pavlov, *Nucl. Phys. B* 52B (Proc. Suppl.) (1997) 17.
- [12] J. Linsley, Proc. 19th ICRC, vol. 7, La Jolla, USA, 1985, p. 193.